

Supplementary Figures

Mutant IDH1-Dependent Chromatin State Reprogramming, Reversibility, and Persistence

Sevin Turcan¹, Vladimir Makarov¹, Julian Taranda², Armida W.M. Fabius^{1, ‡}, Wei Wu¹, Yupeng Zheng³, Nour El-Amine², Sara Haddock^{1, 4}, Gouri Nanjangud⁵, H. Carl LeKaye⁶, Cameron Brennan⁷, Justin Cross⁸, Jason T. Huse¹, Neil L. Kelleher⁹, Pavel Osten², Craig B. Thompson¹⁰, and Timothy A. Chan^{1, 4*}

¹Human Oncology and Pathogenesis Program, Memorial Sloan Kettering Cancer Center, New York, NY 1006

²Cold Spring Harbor Laboratory, Cold Spring Harbor, NY 11724

³Sanofi Genzyme, 153 Second Avenue, Waltham, MA 02451

⁴Weill Cornell School of Medicine, New York, NY 10065

⁵Molecular Cytogenetics Core Facility, Memorial Sloan Kettering Cancer Center, New York, New York 10065

⁶Department of Medical Physics, Memorial Sloan Kettering Cancer Center, New York, NY 10065

⁷Department of Neurosurgery, Memorial Sloan Kettering Cancer Center, New York, New York 10065

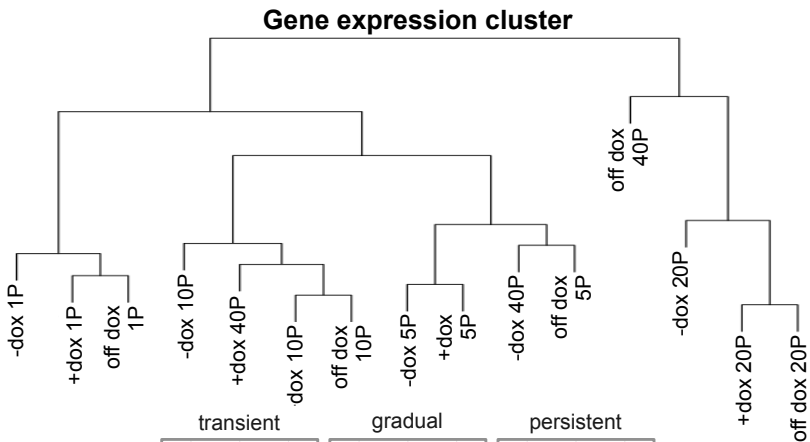
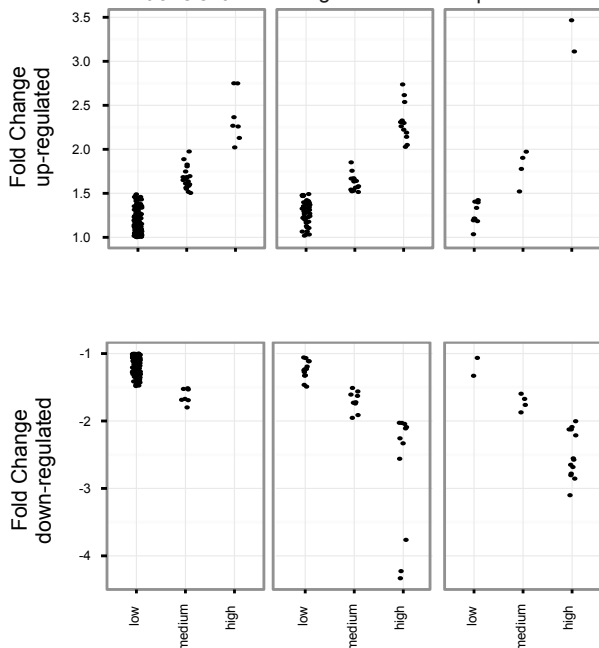
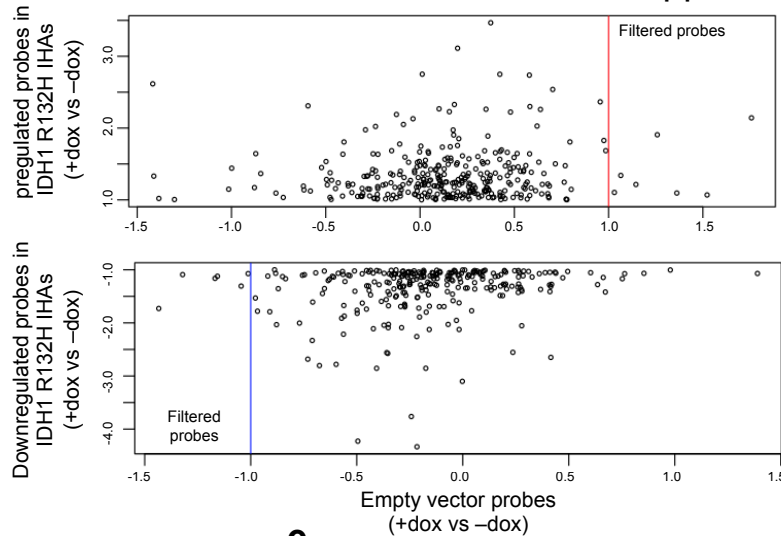
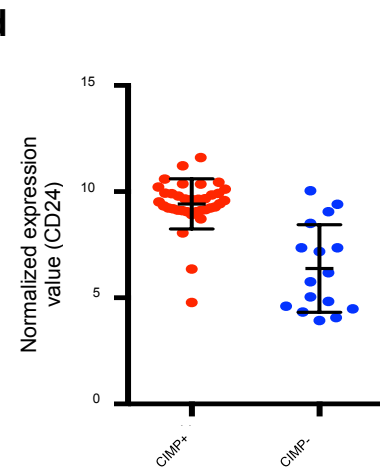
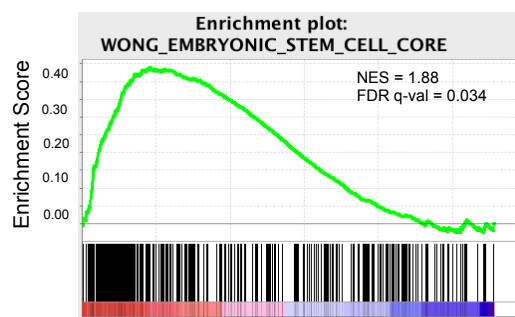
⁸Donald B. and Catherine C. Marron Cancer Metabolism Center, Memorial Sloan Kettering Cancer Center, New York, New York 10065

⁹Departments of Chemistry and Molecular Biosciences, Proteomics Center of Excellence, Northwestern University, Evanston, Illinois 6061

¹⁰Cancer Biology and Genetics Program, Memorial Sloan Kettering Cancer Center, New York, NY 10065

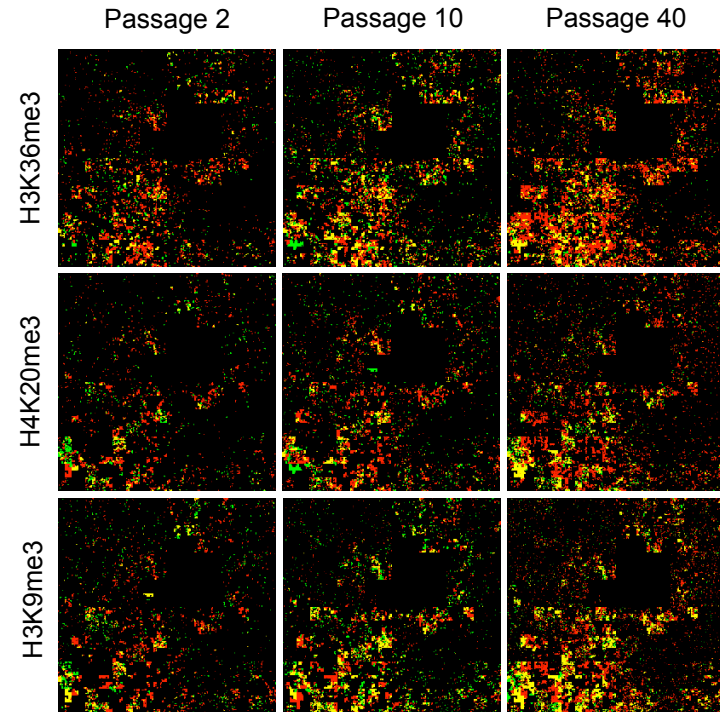
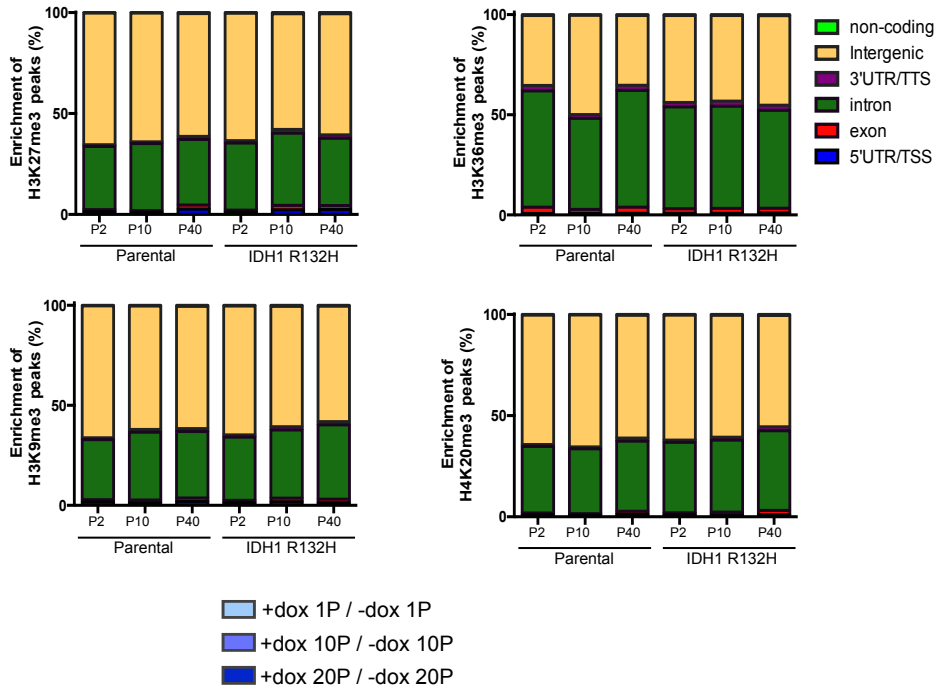
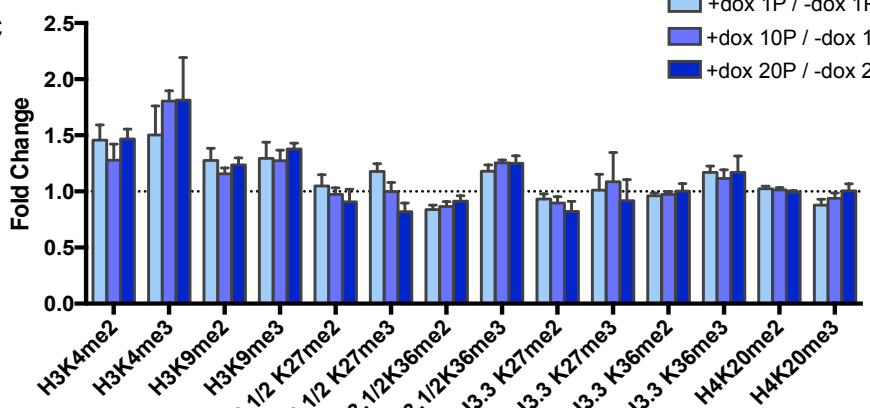
*Correspondence to T.A.C. (chant@mskcc.org)

‡Present address: Department of Ophthalmology, VU Medical Center, Amsterdam, The Netherlands

a**c****b****e****d**

Supplementary Fig. 1 Gene expression kinetics in control immortalized human astrocytes (dox inducible expression of empty vector)

a) Hierarchical clustering of global gene expression profiles in empty vector inducible IHAs, **b)** The y-axis indicates up-regulated probes (gene expression) in IDH1 R132H expressing IHAs, x-axis indicates the corresponding probes in dox inducible empty vector expressing control IHAs. Probes that are either up-regulated >1-fold (red line, top panel) or down-regulated by < -1-fold (blue line, bottom panel) in control astrocytes are filtered from subsequent analyses, **c)** Scatter plot of upregulated genes (top) and downregulated (bottom) (+dox versus -dox at baseline) binned by fold-change across transient, gradual or persistent expression clusters, **d)** Scatterplot of CD24 gene expression in CIMP⁺ and CIMP⁻ lower grade gliomas (n=52), **e)** Gene set enrichment analysis of IDH1 R132H^{CD24⁺} vs IDH1 R132H^{CD24⁻} cells. FDR, false discovery rate; NES, normalized enrichment score.

a**b****c**

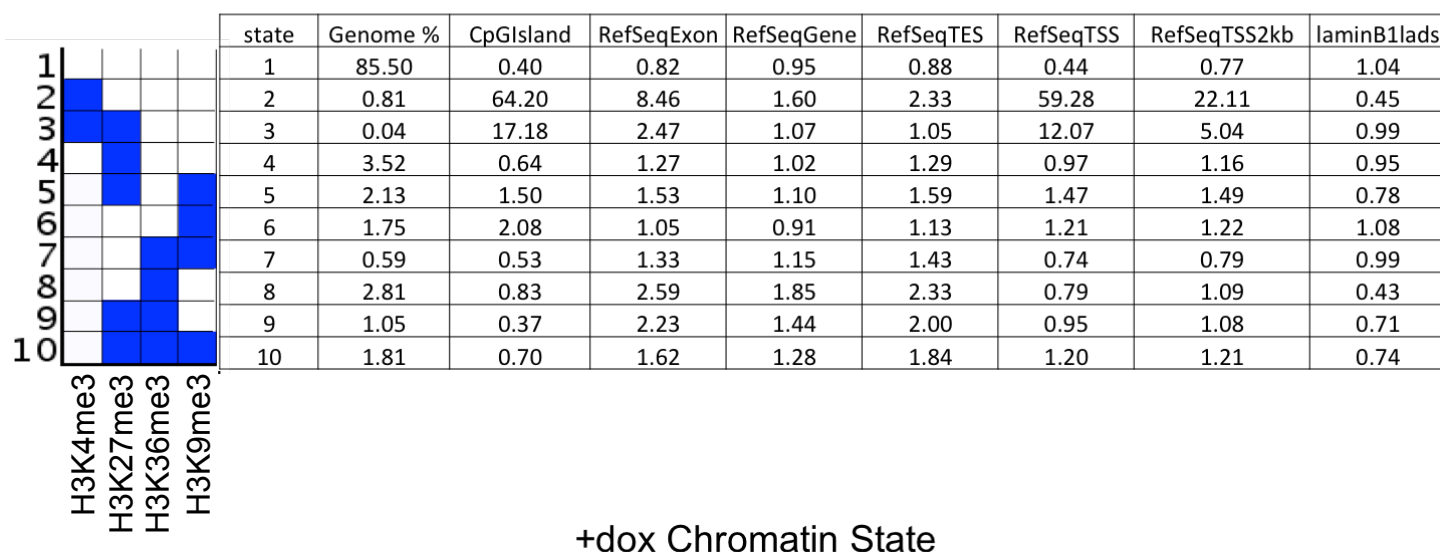
Supplementary Fig. 2

Supplementary Fig. 2 Histone mark landscape in immortalized human astrocytes.

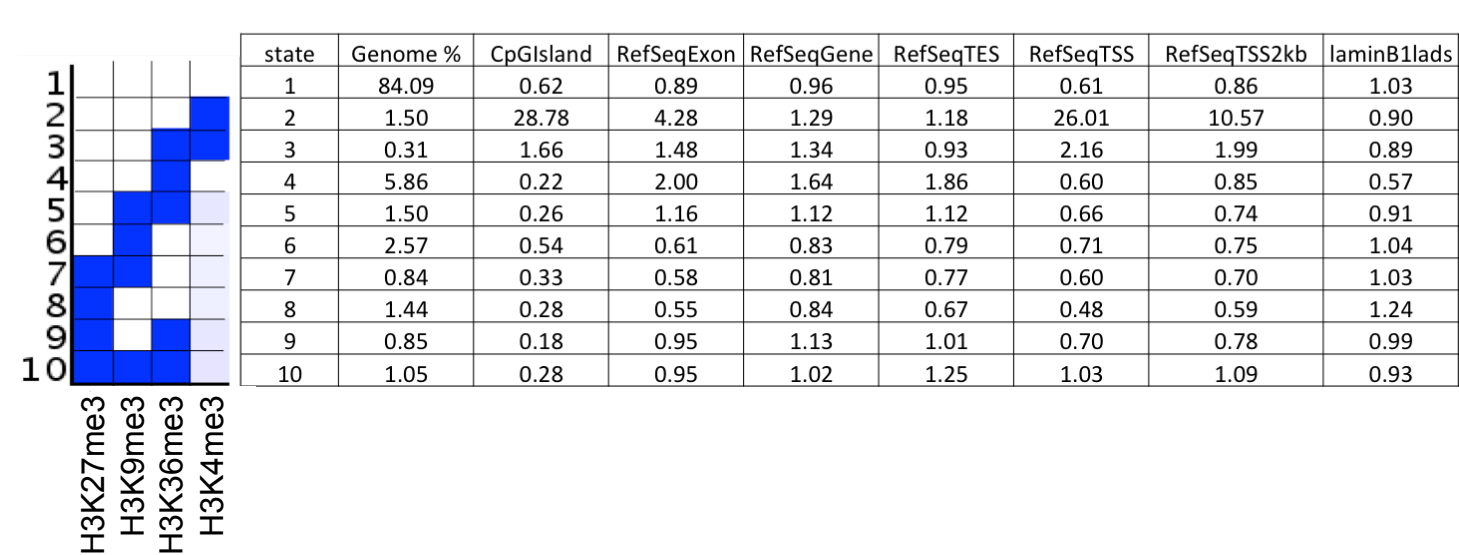
a) Overlapping Hilbert curves (chromosome 1) for H3K36me3, H4K20me3 and H3K9me3 at successive passages of parental pixels (green pixels), IDH1 R132H IHAs peaks (red pixels, constitutive overexpression) and overlapping peaks (yellow), **b)** HOMER derived annotation of genomic loci covered by H3K27me3, H3K36me3, H3K9me3 or H4K20me3 peaks in parental and IDH1 R132H IHAs at passages 2, 10 and 40, **c)** Quantitative liquid-chromatography - mass spectrometry of histone variants and their modifications. Fold change indicates quantitative change in IDH1 R132H +dox samples compared to IDH1 R132H -dox samples at 1, 10 and 20 passages after baseline (passage 30). P, passage; TTS, transcription termination site; UTR, untranslated region

a

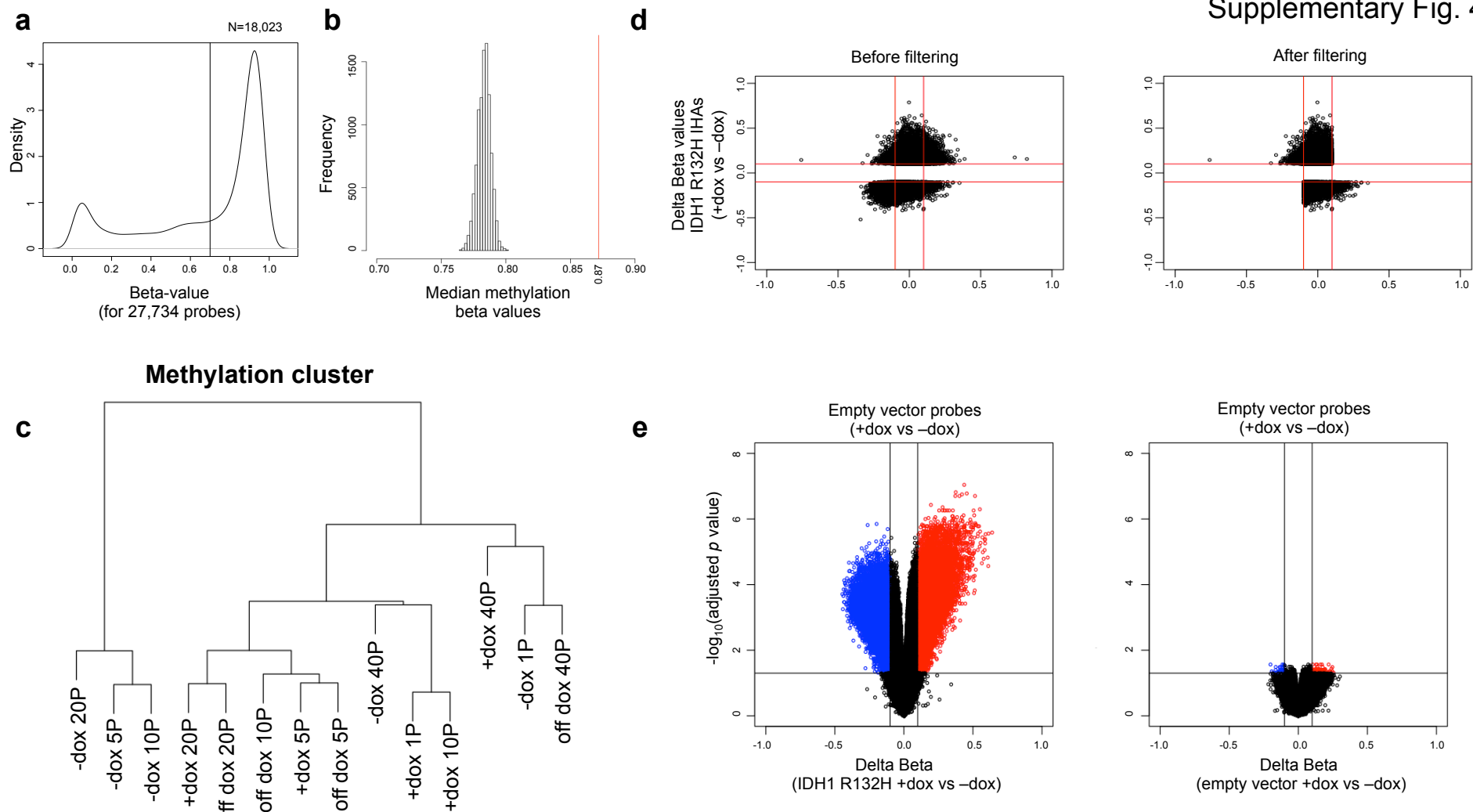
-dox Chromatin State



+dox Chromatin State

**Supplementary Fig. 3. Chromatin states in IDH1 R132H inducible immortalized human astrocytes**

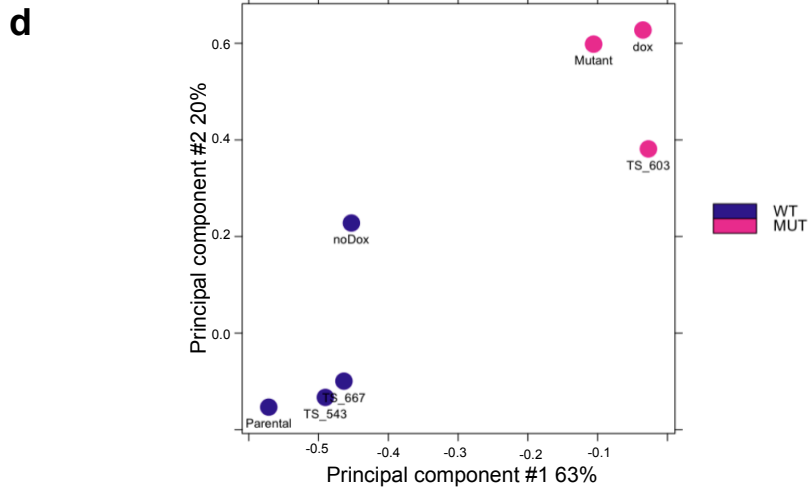
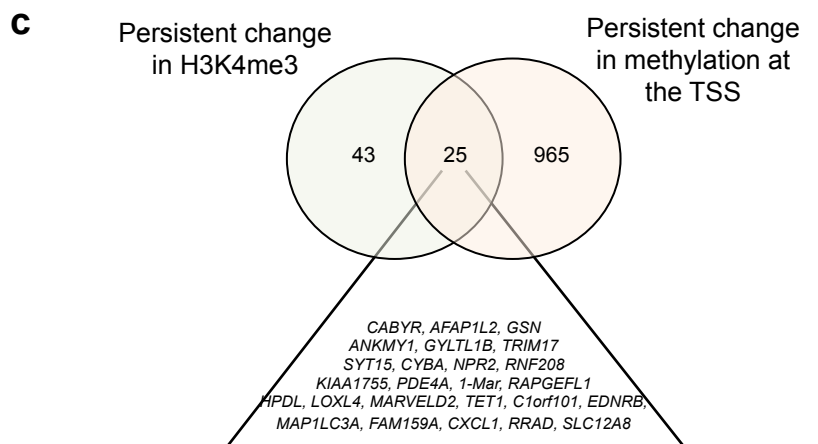
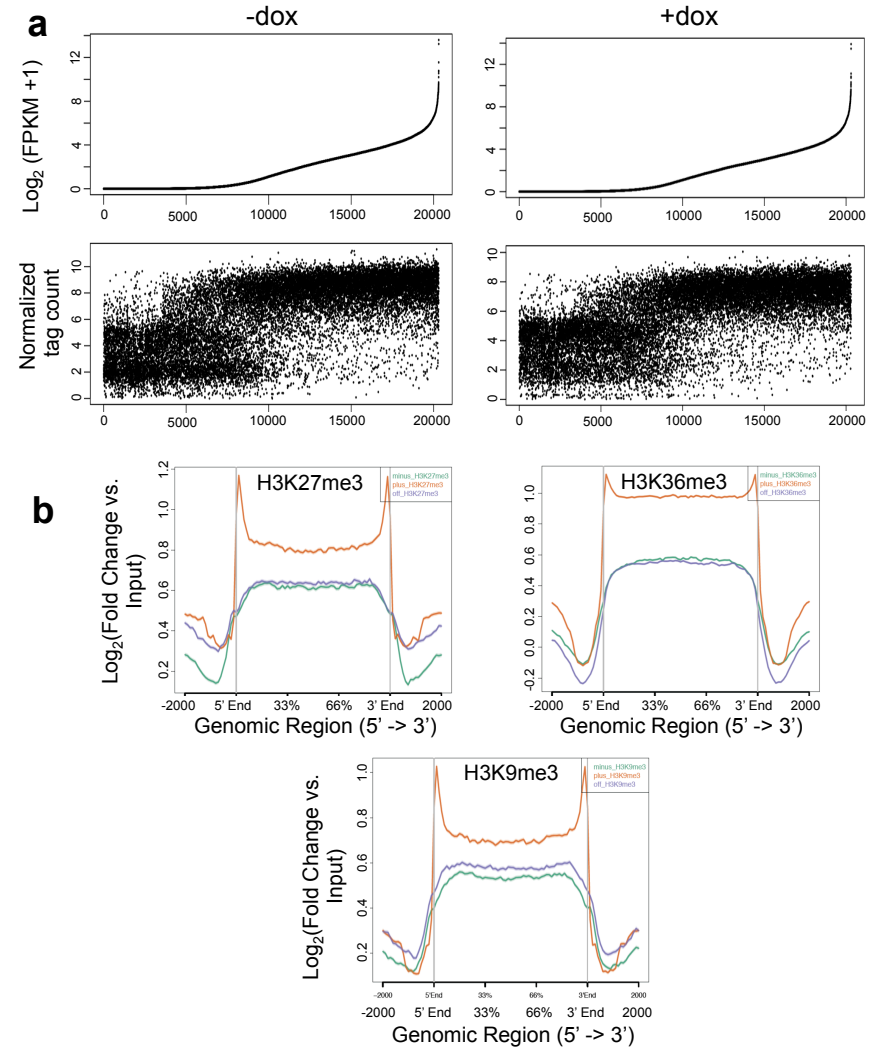
a and b) Chromatin states learned independently for -dox (a) and +dox (b) IDH1 R132H inducible IHAs. Tables show the following features of chromatin states: percent genome covered (Genome %) and overlap with CpG islands (CpGIsland), exons (RefSeqExon), genes (RefSeqGene), transcription end sites (RefSeqTES), transcription start sites (RefSeqTSS), within 2kb of transcription start sites (RefSeqTSS2kb) and lamin B1-associated domains (laminB1lads).



Supplementary Fig 4. Methylation dynamics of inducible immortalized human astrocytes

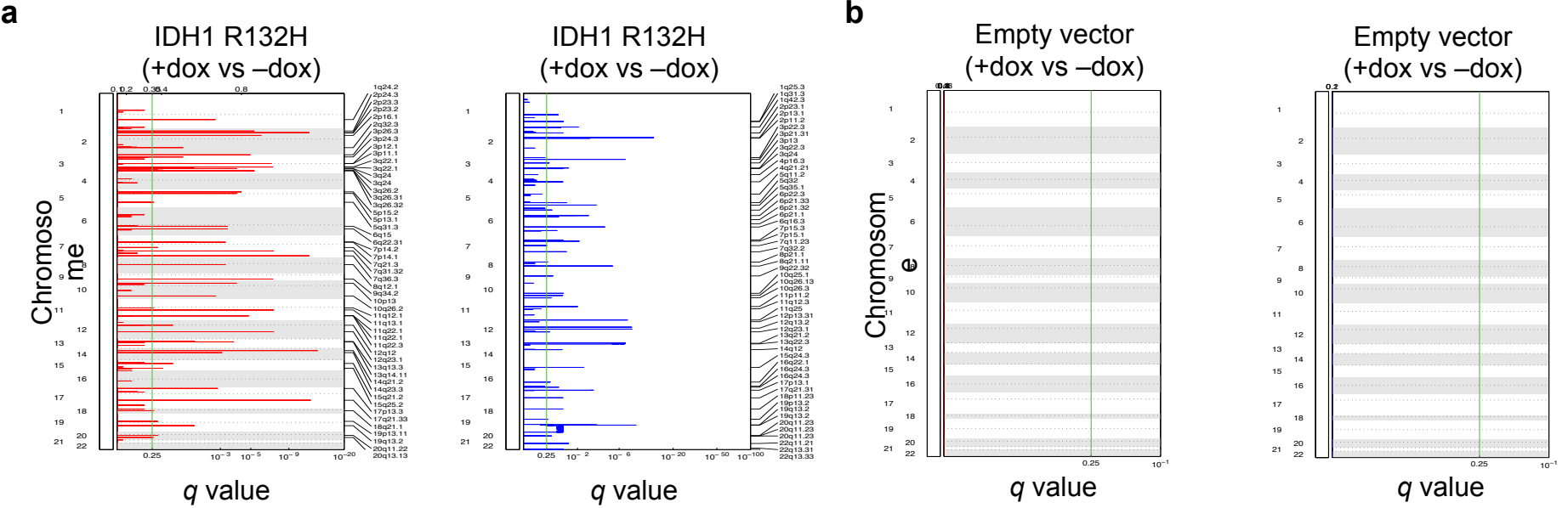
a) Beta-value distribution of 27,734 probes on TS603 glioma tumorspheres with endogenous expression of IDH1 R132H. Probes are derived from hypermethylated probes in IDH1 R132H +dox IHAs compared to -dox IHAs. 18,023 probes display 70% methylation in TS603 cells., **b**) Random set of genes (fixed size of 27,734) were chosen from Illumina 450K probes and median beta value is calculated from TS603 samples. Distribution shows the median beta-value for 10,000 independent random trials and the observed beta value from the hypermethylated loci (median beta value = 0.872) is marked with a red line (p -value < 0.0001), **c**) Hierarchical clustering of global methylation profiles in empty vector inducible IHAs, **d**) y-axis indicates probes with > 0.1 absolute delta beta at baseline passage (passage 30), x-axis indicates the corresponding probes in dox inducible empty vector expressing control IHAs. Probes that display absolute delta beta > 0.1 in control astrocytes are filtered from subsequent analyses (right panel), **e**) Differential methylation analyses across all passages comparing IDH1 R132H +dox vs -dox IHAs (left panel) or empty vector +dox vs -dox IHAs (right panel). Blue dots indicate hypomethylated sites and red dots indicate hypermethylated sites.

Supplementary Fig. 5



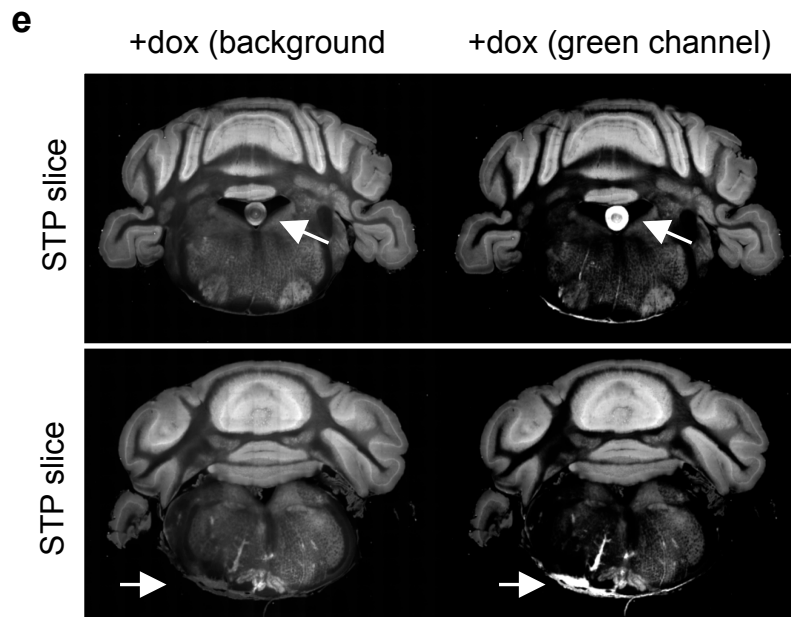
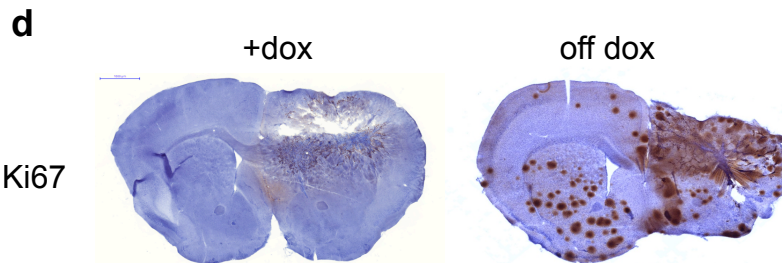
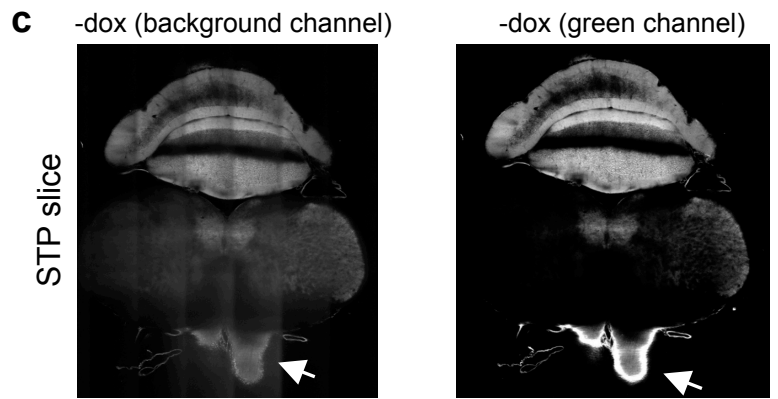
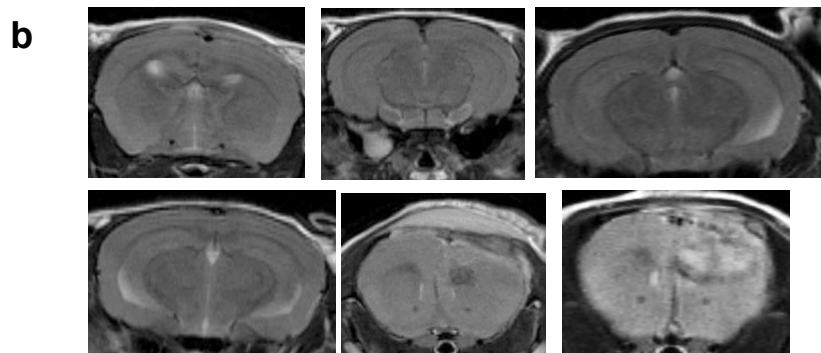
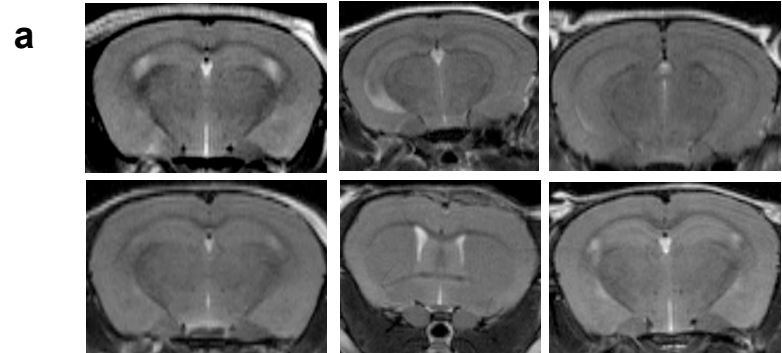
Supplementary Fig. 5. Epigenetic regulation in IDH1 R132H inducible immortalized human astrocytes

a) All genes are sorted in ascending order based on their abundance (FPKM, top panel) as measured by RNA-seq. H3K4me3 enrichment at TSS of FPKM ranked genes are plotted in the bottom panel, **b**) Average profiles of enrichment plots for regions with increased H3K27me3, H3K36me3 or H3K9me3 in IDH1 R132H +dox IHAAs in -dox (green), +dox (orange) and off dox (blue) IHAs, **c**) Overlap of genes with persistent changes in H3K4me3 and methylation at their transcription start sites (TSS) despite long-term withdrawal of dox in IDH1 R132H IHAs, **d**) PCA plot of significant differentially methylated H3K4me3 peaks (1,150 regions) across IDH1 R132H cells (IDH1 R132H stable IHAs at P40, +dox and TS603) compared to IDH wild-type cells (parental at passage 40, -dox, TS543 and TS667). FPKM, fragments per kilobase per million mapped reads; TSS, transcription start site.



Supplementary Fig. 6. Copy number alterations derived from Illumina 450K methylation data

a) GISTIC scores and FDR values (q values; vertical green line is 0.25 cutoff for significance) for amplifications (red lines; left) and deletions (blue lines; right) for IDH1 R132H IHAs are plotted for all chromosomes, **b)** GISTIC scores and FDR values for amplifications (left) and deletions (right) for empty vector IHAs are plotted for all chromosomes. No alterations were detected. FDR, false discovery rate.



Supplementary Fig.7. Characteristics of representative brains orthotopically implanted with IDH1 R132H inducible IHAs.

a and b) Representative T2-weighted MR images (axial brain slices, 6 mice per group) for control IHAs (a) and IDH1 R132H IHAs (b) 5-months post injection, **c)** Representative STP slice for a control mouse (-dox) without discernible tumor on MRI, but cellular growth as evidenced by green fluorescence (ZsGreen) detection in the hindbrain (white arrows), **d)** Representative Ki67 stain for an IDH1 R132H +dox and an off dox (dox withdrawn) brain, **e)** Representative STP slice for +dox mice showing cellular growth in the hindbrain region (green channel).